

Excitons in charged Ge/Si type-II quantum dots

A I Yakimov[†]§, N P Stepina[†], A V Dvurechenskii[†], A I Nikiforov[†]
and A V Nenashev[‡]

[†] Institute of Semiconductor Physics, Siberian Branch of the Russian Academy of Sciences,
630090 Novosibirsk, Russia

[‡] Novosibirsk State University, 630090 Novosibirsk, Russia

E-mail: yakimov@isp.nsc.ru

Received 3 July 2000, in final form 5 September 2000, accepted for publication 19 September 2000

Abstract. Using electron-filling modulation absorption spectroscopy, we study the effect of quantum dot (QD) charging on the interband excitonic transitions in type-II Ge/Si heterostructures containing pyramidal Ge nanocrystals. In contrast to type-I systems, the ground-state absorption is found to be blueshifted when exciton–hole and exciton–exciton complexes are formed. We argue that this is the consequence of dominance of the hole–hole and electron–electron interactions compared to the electron–hole interaction due to the spatial separation of the electron and hole. The large oscillator strength (0.5) and the exciton binding energy (25 meV) are estimated from the experimental data. The results are explained by effects of the electron and hole localization and by electron wavefunction leakage in the dots. The electronic structure of spatially indirect excitons is calculated self-consistently in the effective-mass approximation for pyramidal-shaped Ge/Si QDs. The inhomogeneous strain distribution in the QD layer has been taken into account through modification of the confining potential. The calculations show that the electron of an indirect exciton resides in the Si near to the Ge pyramid apex due to maximum strain in this region, while the hole is confined close to the pyramid base. The electron–hole overlap is determined to be 15%. A satisfying agreement is found between all theoretical and experimental data.

1. Introduction

The study of the excitonic properties in quantum-dot (QD) structures has drawn considerable interest in recent years. Most of the work has been reported in the type-I QD structures, where an electron and a hole are confined spatially in the same quantum well. Ge/Si(001) QDs exhibit a type-II band lineup. The large (~ 0.7 eV) valence-band offset characteristic of this heterojunction leads to an effective localization of holes in Ge regions, which represent potential barriers for electrons. When an electron–hole pair is photoexcited, the hole is captured by the Ge dot and creates a Coulomb potential, resulting in a binding of an electron in the vicinity of the Ge dot (figure 1). The spatially separated interacting electron and hole are usually referred to as an ‘indirect exciton’ [1–5]. Intriguing properties of indirect excitons are still poorly understood. In particular, little is known about the influence of Coulomb interactions on the excitonic properties of charged QDs.

Usually, the excitonic transitions in Ge/Si self-assembled islands are studied by photoluminescence (PL) spectroscopy [3, 6, 7]. Typical dot sizes in the cited papers range between 70 and 300 nm, i.e. about one order of magnitude larger than those of our sample (see below). Such

§ Corresponding author.

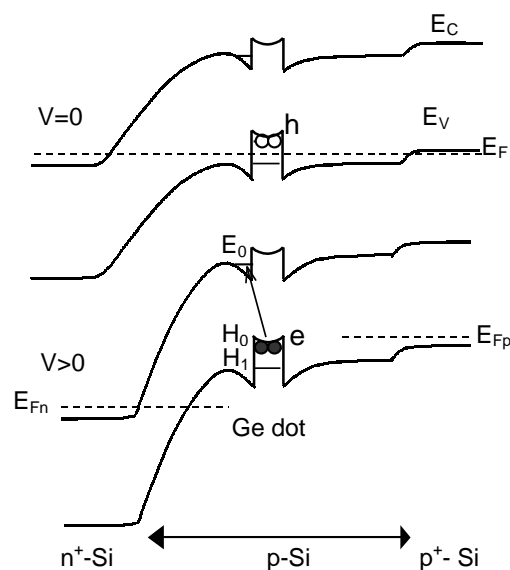


Figure 1. Schematic band diagram of the investigated sample under unbiased and reverse biased conditions.

dots do not represent a real zero-dimensional system as the carrier wavefunctions in the dots have a large extent. For the same reason, the electron–hole interaction is very small in

these systems, and thus the excitonic nature of the dot PL is questionable.

In this paper, we use electron-filling modulation absorption spectroscopy (EFA) to study the effect of dot charging on the interband transitions in 10 nm scale Ge/Si QDs. Previously, this kind of spectroscopy has been successfully used to study PL [8] and reflectance [9] properties of charged InAs and $\text{In}_x\text{Ga}_{1-x}\text{As}$ QDs. In the present experiments, Ge dots are embedded into an n^+p-p^+ Si diode, in which the number of holes in the QDs can be finely tuned by an external applied bias. When a state is occupied by a hole, no interband transition from this state is possible (figure 1). When the hole is evacuated from the level, the interband transition is allowed. Modulating the holes in and out of the state by applying an ac bias voltage therefore induces corresponding changes in the infrared absorption. Thus the absorption signal measured under different bias conditions reflects directly properties of excitons at charged QDs.

2. Samples and experiment

The sample was grown by molecular beam epitaxy on a (001) oriented 4.5 Ω cm boron doped Si substrate. The growth temperatures for the silicon layers were 800 and 500 $^\circ\text{C}$ before and after deposition of the Ge layer, respectively. The growth rates were 2 ML s^{-1} for Si and 0.2 ML s^{-1} for Ge. The Ge QD layer with a nominal thickness of 10 ML was symmetrically embedded into a 1 μm thick p-Si region ($B, 5 \times 10^{16} \text{ cm}^{-3}$) at 300 $^\circ\text{C}$. A buried back contact is formed by 50 nm B doped p^+ -Si ($2 \times 10^{18} \text{ cm}^{-3}$). The structure was finally capped with a 50 nm n^+ -Si front contact ($\text{Sb}, 1 \times 10^{19} \text{ cm}^{-3}$). The formation of the Ge QDs was indicated by observing the change in the reflection electron diffraction pattern from streaky to spotty. The structures of similar samples were examined, before deposition of the Si cap layer by scanning tunnelling microscopy, and after overgrowth of the cap layer by cross-sectional transmission electron microscopy [10]. The dots are pyramidal with base orientation along [100] and [010] directions. The area density of the dots was estimated to be $3 \times 10^{11} \text{ cm}^{-2}$. The average size of the dot base length was found to be about 15 nm, the height about 1.5 nm and the dot uniformity approximately $\pm 20\%$.

Infrared absorption measurements were performed in normal-incidence geometry on mesa diodes at room temperature. Unmodulated light from a global source illuminated the front side of the diode. The transmitted light then passed through the monochromator and was detected by a Ge photodiode. Differential absorption was measured by applying a reverse bias modulated between a low level V_L and a high level V_H .

The 100 kHz capacitance–voltage (C – V) characteristic measured at 300 K is shown in figure 2(a) and illustrates the charge state of the sample investigated. The region of negative slope in the C – V curve (at $V_H = 6$ –8 V) is a consequence of the zero dimensionality of states associated with the dots [11]. To determine the position of the QD layer we used the approximate relation $x = \epsilon_0\epsilon_r/C$, where ϵ_r is the relative permittivity. For $C \approx 20 \text{ nF cm}^{-2}$, the result

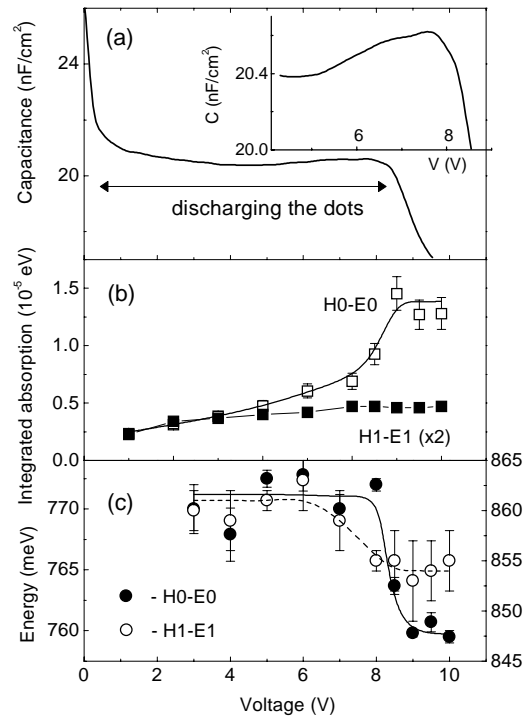


Figure 2. (a) C – V characteristic measured at $T = 300$ K with a modulation amplitude 10 mV and a modulation frequency 100 kHz. (b) Integrated absorption strength of the H0–E0 and H1–E1 transitions as a function of bias voltage V_H . (c) Energetic position of the ground-state (left axis) and excited-state (right axis) excitonic transitions in the dark versus applied bias V_H . Curves in (b) and (c) are guides for the eye.

is $x = 0.5 \mu\text{m}$, which is in agreement with the nominal position of the Ge layer. The dots are charged with holes at zero bias. The holes begin to escape at $V_H > 0.5$ V and the dots become totally depleted at $V_H > 8.5$ V (figure 2(a)). In the discussion that follows, we modulate the bias voltage between $V_L = 0$ V and $V_H = 2$ –10 V. All measured EFA signals were normalized to the source spectrum so that any spectral response not associated with the modulated part of the sample is eliminated from the results. This approach is appropriate for the case of weakly absorbing samples.

3. The interband absorption

Figure 3 shows the EFA signal measured at different values of the bias V_H . Below the energy gap of Si, at energies 650–850 meV, we observe an absorption maximum with a broadening of ~ 50 –70 meV. In figure 4 we show that this maximum can be well described by a sum of two Gaussian peaks. The symmetric line shape of the two peaks is characteristic of a bound-to-bound transition. We interpret the first absorption peak as an excitonic transition between the hole ground state (H0) in the Ge dots and the electron ground state (E0) confined in Si near the heterojunction. A similar peak at ~ 730 –750 meV has been observed previously in photocurrent spectra of a Ge/Si heterostructure with QDs of similar size [10]. A second maximum at ≈ 860 meV is assigned to the excited-state excitonic transition (the H1–E1 transition). We assume that the broadening of the interband

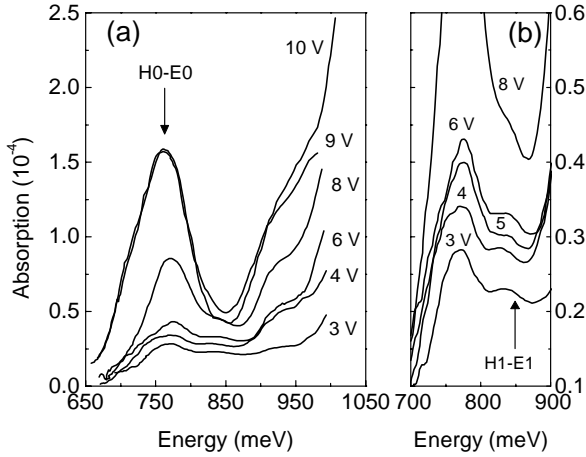


Figure 3. (a) Room-temperature electron-filling absorption spectra at different reverse bias. (b) Expanded view of the spectra at low bias.

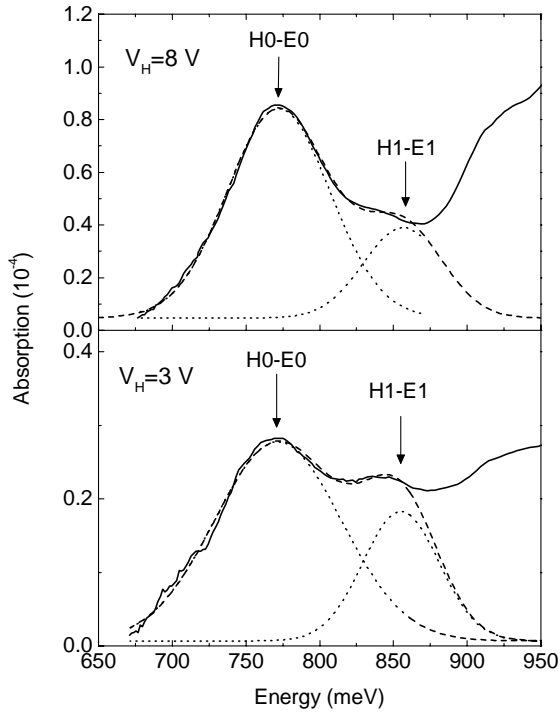


Figure 4. Low-energy absorption spectra for two bias voltages. Solid curves show the experimental data; dotted curves give the result of decomposition into Gaussians.

transitions is mainly due to the dispersion of the carrier confinement energies of dots with different sizes.

At higher energies, the absorption gradually increases due to excitations to extended states in the conduction band of Si and Ge, superimposed on the several absorption bumps, which are tentatively attributed to transitions between highly excited states in the dots or in the wetting layer. To make a careful analysis of the absorption edges, one should take into account the energy dependence of absorption coefficient for spatially indirect transition from a confined state to a delocalized band. Since a theoretical treatment of such a dependence is a formidable task, we will not make this analysis in this paper.

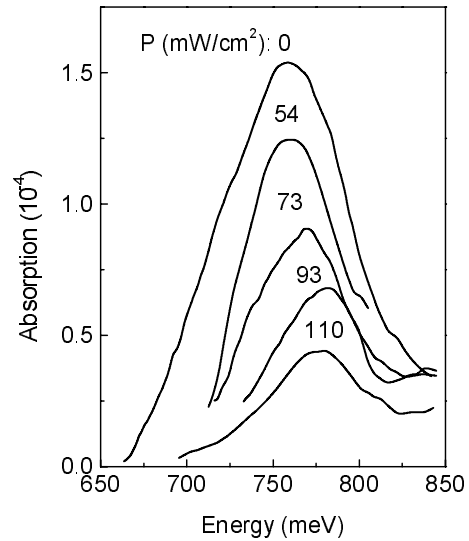


Figure 5. Effect of optical pumping on the EFA spectra at different pump intensities. The modulation bias amplitude is fixed at $V_H = 9$ V.

The assignment of the peaks near 760–770 and 855–860 meV to the H0–E0 and H1–E1 transitions, respectively, is supported by analysis of the integrated absorption I as a function of V_H (figure 2(b)). (I is obtained by calculating the areas under Gaussians fitted to the absorption peaks.) In our geometry

$$I = \frac{he^2nf}{2m_0\epsilon_0c} (1 + \sqrt{\epsilon_r}), \quad (1)$$

where n is the density of electrons in the highest valence band state of the Ge dots, f is the oscillator strength and c is the speed of light. Since $I \propto n$, the I – V_H curve illustrates the change in the charge state of the dots. At $V_H > 8.5$ V, the integrated H0–E0 absorption does not depend on the voltage. Below 8.5 V, the EFA intensity weakens, indicating a decrease in the number of modulated electrons in the valence band of the dots, in agreement with the C – V measurements. Note that the integrated absorption strength of the H1–E1 transition does not show significant voltage dependence when going from 10 to 4 V because there are still no holes in the excited state at this point.

To obtain further evidence to support the proposed origin of the EFA peak, we have studied the effect of additional interband optical excitation of the sample by a tungsten halogen lamp with a bandpass filter as the source. The absorption spectra obtained at a fixed modulation voltage ($V_H = 9$ V) and at different pump excitation densities are depicted in figure 5. When the sample is illuminated, nonequilibrium electrons and holes are photogenerated. The holes are captured by the dots while the electrons are accumulated near the dots, forming the indirect excitons. At high pump intensities, the hole and electron ground states become fully occupied and the Pauli exclusion principle forbids the H0–E0 transition. One can see in figure 5 that the experimental EFA signal is strongly suppressed by the optical pumping.

The integrated absorption at $V_H > 8.5$ V can be used to determine the oscillator strength per dot. For the H0–E0 transition, the density of absorbers is twice the dot

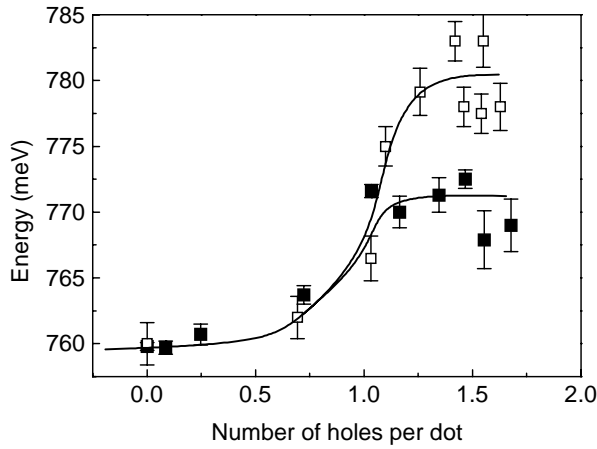


Figure 6. Ground-state transition energy as a function of the hole occupation per dot. The data were taken at different biases in the dark (solid squares), and at different pump intensities at fixed bias voltage ($V_H = 9$ V, open symbols).

density. (The maximum occupation of the ground state is 2.) From the measured value $I \simeq 1.4 \times 10^{-5}$ eV we find $f = 0.5$. This value is less than 1/20th of that obtained for direct excitons in InAs/GaAs QDs (10.9) [12]. Such a difference is not unreasonable since the difference between the two types of QD is large. Similar conclusions were reached [4] from analysis of the PL time decay of type-II GaSb/GaAs QDs. Large values of the oscillator strength and the exciton binding energy for type-II QDs with finite offsets was predicted by Rorison [13]. They are explained by two aspects of the system. The first is the localization of one of the particles which allows the other particle of the exciton to correlate more strongly with it. The second is leakage of the wavefunctions into the barrier regions allowing greater overlap of electron and hole wavefunctions.

4. Shift of the excitonic transition

One of the main results is that the H0–E0 transition shows a substantial stepwise blueshift of about 11 meV with decreasing reverse bias (figure 2(c)). A qualitatively similar effect is seen with increasing the pump excitation density at fixed V_H (figure 5). This result differs drastically from what has been observed for direct excitons, in which case charging leads to a redshift of the excitonic transition [8, 12]. It can be seen in figure 2(c) that the transition energy begins to increase when holes are injected into the originally empty QDs. From the oscillator strength obtained above and the measured integrated absorption we calculate the number of holes per dot, N_h , at different biases in the dark and at different pump intensities. The energetic position of the indirect excitonic transition is shown in figure 6 as a function of N_h . It should be noted that the transition energy increases sharply when the first hole enters the ground state and then is approximately insensitive to further increase in the hole concentration.

The QDs are located in the space-charge region of a pn-diode and, therefore, are subjected to a relatively strong electric field. As is well known from the quantum confined Stark effect (QCSE), an electric field can affect the energetic

position of QDs states. We find three arguments against interpretation of the experimental data in terms of the QCSE. First, the Stark shift should be continuous with the field strength. However, we observe that the position of the absorption changes sharply at 8.5 V and then is constant at higher bias. Second, a field-induced energy shift should be weak since the height of the QDs in the field direction is only 1.5 nm. Recently Miesner *et al* [7] have observed a QCSE of about 60–70 meV at 5 V for 7.5 nm height Ge/Si QDs. Since the dependence of the QCSE on the width w of the quantum well is established to be very strong ($\sim w^4$ [14]), we expect only a negligible Stark shift of ≈ 0.1 meV in the investigated sample. Third, when the external electric field is increased in Ge/Si QDs, a blueshift of the excitonic transition is expected from the experiments of Miesner *et al* [7]. However, we observe a redshift with increasing bias voltage (figure 2(c)). Thus we conclude that charging and not the QCSE is responsible for the observed energy shift.

When a H0–E0 exciton is created in a positively charged dot, an exciton–hole complex is formed, consisting of two holes in the dot and an electron confined near the dot. There are two additional contributions to the energy of the exciton–hole complex as compared to e–h excitation in a neutral dot [12]. The first is a positive Coulomb energy due to correlation between the two holes in the dot, E_{hh} , and the second is a negative contribution from the Coulomb attraction between the excited electron in the nearby silicon and the second hole on the dot, E_{eh} . Here we neglect the exchange interaction between the two holes since they have antiparallel spin orientation [15]. For direct excitons, the electron–hole interaction dominates and the resulting shift $\Delta E_{h-ex} = E_{hh} - E_{eh}$ is negative [12]. Hence the expected reduction of the overlap factor for type-II excitons as compared with type-I systems yields a smaller magnitude of the electron–hole interaction energy E_{eh} . As a result, the energy of the exciton–hole interaction referenced to a neutral exciton energy can be positive. Taking the experimentally observed shift of 11 meV and $E_{hh} = 36$ meV [11], the exciton binding energy is estimated to be $E_{eh} = 25$ meV. Note that this value is larger than the free-exciton binding energy in the bulk Si (≈ 10 meV), in agreement with Rorison’s arguments [13].

As can be seen from figure 6, optical pumping affects the transition energy more strongly than the bias voltage. This stems from the fact that illumination creates both holes and electrons while the field effect only induces holes in the dots. Under illumination we have two interacting excitons in the dot: the first is generated by the pump illumination, the second is excited by the infrared probing light. As compared to a single exciton, the transition energy now increases by $\Delta E_{ex-ex} = E_{ee} + E_{hh} - 2E_{eh}$, where E_{ee} is the energy of repulsive interaction between two electrons confined near the dot.

It is of importance that the excited-state absorption is less changed when the hole enters the ground state. This can be easily understood in the context of our scenario. As the wavefunction overlap is reduced, Coulomb interaction between holes in the ground state and in the excited state is smaller than interaction between two holes in the ground state [12]. Therefore, the excited-state excitonic transition is expected to be less sensitive to carrier–carrier interaction.

Table 1. Energy parameters of indirect exciton and excitonic complexes in Ge/Si QDs. E_1 is the electron localization energy for a single exciton, E_{eh} the exciton binding energy and ΔE_{ex-h} and ΔE_{ex-ex} are the shifts of the excitonic transition for the exciton–hole and exciton–exciton complexes as compared to a single exciton.

Source	E_1 (meV)	E_{eh} (meV)	ΔE_{ex-h} (meV)	ΔE_{ex-ex} (meV)
Experiment	—	25	+11	+20
Calculation	38	31	+9.7	+10.2

5. Self-consistent calculations

To obtain theoretical estimates of the oscillator strength and all Coulomb energies of the system under investigation, a realistic Ge nanocrystal geometry has to be used for model calculations. We consider a $\{105\}$ -faceted Ge pyramid with a square base in the (001) plane and with base length of 15 nm and height of 1.5 nm. The nanocrystal rests on a 5 ML thick Ge wetting layer and is entirely surrounded by Si. In the discussion that follows, the z -axis is taken to be along the principal axis of symmetry of the pyramid. The x and y axes lie in the plane of the wetting layer. First of all, the strain distribution inside and around the QD was calculated using the valence force field (VFF) model with the Keating potential [16]. The VFF model is a microscopic theory which includes bond stretching and bond bending, and avoids the potential failure of elastic continuum theory in the microscopic limit. Then the strain-induced modifications of the conduction and valence bands of Ge and Si were obtained by using deformation potentials given in [17]. As a result of strain, the sixfold degeneracy of the conduction-band minima in Si is lifted to give two lowest Δ minima, oriented along $[001]$ and $[00\bar{1}]$ directions and lying lower than those in Ge. In order to investigate the excitonic properties, a set of three-dimensional self-consistent effective-mass Schrödinger equations was solved for electrons and holes using the Hartree approximation. The set contains two equations for a single exciton, three equations for an exciton–hole complex and four equations for two excitons at the dot. The interaction between charged particles was modelled by a statically screened Coulomb potential: $U_{ij}(r_i, r_j) = e^2/4\pi\epsilon\epsilon_0|r_i - r_j|$. In the conduction band, the band offset between Δ minima of unstrained Ge and Si is taken to be equal to 340 meV. In the valence band, the band offset without strain is 610 meV. The effective mass in both the conduction and valence bands is decoupled between the growth axis and the layer plane. The effective mass in the conduction band of Si is $m_z = 0.92m_0$ and $m_{xy} = 0.19m_0$. In the valence band of Ge, the effective mass is taken to be equal to $m_z = 0.2m_0$ and $m_{xy} = 0.39m_0$. Only the heavy-hole states are considered in the valence band, since the light-hole states lie close to the valence-band edge.

The experimental and calculated values of exciton energies are listed in table 1. One can see a good agreement between calculations and experiment along the rows. The calculated electron localization energy $E_1 = 38$ meV consists of two contributions: the first one comes from localization in the strain-induced potential well (7 meV), the second one is due to electron–hole interaction (31 meV). The latter value is in agreement with the exciton binding energy estimated from experiment (25 meV). The confining potentials for the electron and hole along the z -axis in the structure and the

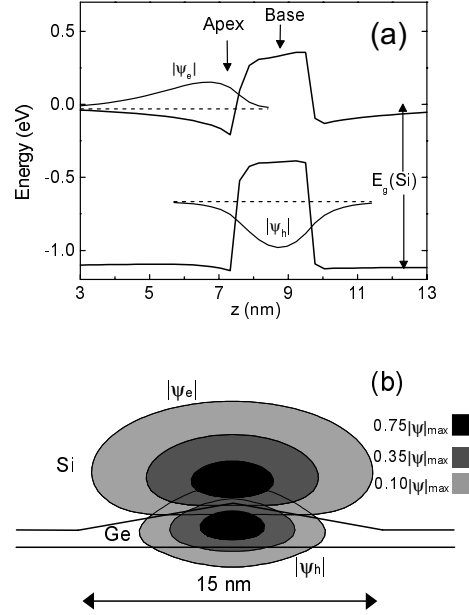


Figure 7. The confining potentials and the wavefunctions for the electron and heavy hole along the principal axis of symmetry in the dot (a). Isosurface plots of the electron and hole states (b).

carrier wavefunctions are given in figure 7(a). Figure 7(b) shows the isosurfaces of the electron and hole wavefunctions. Note that the electron is localized near the pyramid apex, where the strain is a maximum. The electron–hole overlap is calculated to be 15%. If we take an electron–hole overlap of 80% for type-I InAs/GaAs QD [18] and an oscillator strength of 10.9 as observed also for InAs/GaAs [12], we expect for the dots with an electron–hole overlap of 15% an oscillator strength of about 0.38, in reasonable agreement with experiment. This large oscillator strength of the Ge QDs can be explained by electron leakage in the dots.

6. Conclusions

We have used electron-filling modulation absorption spectroscopy to study the interband transitions in charged type-II Ge/Si QDs. When the dots are loaded with holes by changing the reverse bias, the ground-state transition in the absorption spectra shows a stepwise blueshift of about 11 meV accompanied by a decrease in intensity. Interband optical pumping at a fixed bias voltage leads to a shift of about 20 meV. The observed changes are explained by exciton–hole and exciton–exciton interactions. Based on the absorption measurements, we have estimated the exciton oscillator strength $f = 0.5$ and the exciton binding energy 25 meV. The experimental results are well supported by our detailed self-consistent calculations.

Acknowledgments

The authors would like to acknowledge very useful discussions with John Adkins from Cambridge University. This work was supported by the Russian Foundation of Basic Research (grant no 99-02-17019), the Interdisciplinary Scientific and Technical Programme ‘Physics of solid state nanostructures’ (grant no 98-1100) and the Intercollegiate Scientific Programme ‘Universities of Russia—basic research’ (grant no 015.01.01.34).

References

- [1] Branis S V and Bajaj K K 1992 *Phys. Rev. B* **45** 6271
- [2] Ledentsov N N *et al* 1995 *Phys. Rev. B* **52** 14 058
- [3] Fukatsu S, Sunamura H, Shiraki Y and Komiyama S 1997 *Appl. Phys. Lett.* **71** 258
- [4] Hatami F *et al* 1998 *Phys. Rev. B* **57** 4635
- [5] Kalameitsev A B, Kovalev V M and Govorov A O 1998 *JETP Lett.* **68** 669
- [6] Sunamura H, Usami N, Shiraki Y and Fukatsu S 1995 *Appl. Phys. Lett.* **66** 3024
- Palange E, Capellini G, Di Gaspare L and Evangelisti F 1996 *Appl. Phys. Lett.* **68** 2982
- Liu F and Lagally M G 1997 *Surf. Sci.* **386** 169
- Rodrigues P A M, Cerdeira F and Bean J C 1999 *Appl. Phys. Lett.* **75** 145
- [7] Miesner C, Röthig O, Brunner K and Abstreiter G 2000 *Physica E* **7** 146
- [8] Schmidt K H, Medeiros-Ribeiro G and Petroff P M 1998 *Phys. Rev. B* **58** 3597
- [9] Hsu T M, Chang W H, Tsai K F, Chyi J I, Yeh N T and Nee T E 1999 *Phys. Rev. B* **60** R2189
- [10] Yakimov A I, Dvurechenskii A V, Proskuryakov Yu, Nikiforov A I, Pchelyakov O P, Tey S A and Gutakovskii A K 1999 *Appl. Phys. Lett.* **75** 1413
- [11] Yakimov A I, Dvurechenskii A V, Nikiforov A I and Pchelykov O P 1998 *JETP Lett.* **68** 135
- [12] Warburton R J, Dürr C S, Karrai K, Kotthaus J P, Medeiros-Ribeiro G and Petroff P M 1997 *Phys. Rev. Lett.* **79** 5282
- [13] Rorison J M 1993 *Phys. Rev. B* **48** 4643
- [14] Bastard G, Mendez E E, Chang L L and Esaki L 1983 *Phys. Rev. B* **28** 3241
- [15] Wojs A and Hawruluk P 1997 *Phys. Rev. B* **55** 13 066
- [16] Nenashev A V and Dvurechenskii A V 2000 *JETP* **91** 497
- [17] Van de Walle C G 1989 *Phys. Rev. B* **39** 1871
- [18] Grundmann M, Stier O and Bimberg D 1995 *Phys. Rev. B* **52** 11 969